TÜBİTAK

Turkish J. Eng. Env. Sci.
36 (2012) , 33 – 44.

doi:10.3906/muh-1010-28

Electromagnetomechanical responses of a radially polarized rotating functionally graded piezoelectric shaft

Ali GHORBANPOUR ARANI[1,*], Reza BAKHTIARI[1], Mehdi MOHAMMADIMEHR[1], Mohammad Reza MOZDIANFARD[2]

[1] *Department of Mechanical Engineering, Faculty of Engineering, University of Kashan, Kashan, I.R. IRAN*

e-mails: aghorban@kashanu.ac.ir, a_ghorbanpour@yahoo.com

[2] *Department of Chemical Engineering, Faculty of Engineering, University of Kashan, Kashan, I.R. IRAN*

Received: 25.10.2010

Abstract

In this article, electromagnetomechanical responses of a radially polarized rotating shaft made from functionally graded piezoelectric material (FGPM) and subjected to a uniform magnetic field with mechanical loads and electric potentials are investigated. All material, electrical, and magnetic properties were assumed to follow an identical power law in the radial direction. Exact solutions for electric displacement, stresses, electric potentials, and perturbation of the magnetic field vector are presented using the infinitesimal theory of electromagnetoelasticity. Numerical results showed that responses were strongly affected by power law index β. We could optimize the responses by manipulating β, electric potential, and magnetic field intensity.

Key Words: FGPM, electromagnetoelastic, hollow cylinder, radially polarized, perturbation of magnetic field vector

1. Introduction

In recent years, advances made in material research have greatly supported other engineering disciplines. Composite materials like functionally graded materials (FGMs) offer desirable heat transfer, corrosion, and fracture resistance properties and are considered advanced materials and good substitutions for alloys. Developments in the smart-structure technology of FGMs and the characteristics mentioned above have yielded functionally graded piezoelectric materials (FGPMs) that could be used as sensors and actuators in engineering applications.

As far as FGPM development is concerned, the axial vibration of long piezoelectric homogeneous cylinders was considered by Adelman et al. (1975). Later, Chen (1999) simplified the governing differential equations of radially polarized piezoelectric cylinders to ordinary Euler differential equations, using the displacement function. Wu et al. (2002) presented a high-order theory to examine the electromechanical behavior of piezoelectric generic shells with FGM properties in the thickness direction. Jabbari et al. (2002) developed

*Corresponding author

a general analysis of one-dimensional steady-state thermal stresses in a hollow, thick cylinder made of FGM. They used a direct method to solve the heat conduction and Navier equations, assuming all material properties as power functions of the radius except Poisson's ratio. Kwon and Lee (2004) studied the dynamic response of a cracked FGPM subjected to transient antiplane shear mechanical load and in-plane electrical load. By using Laplace and Fourier transforms, they reduced their analysis to the solutions of Fredholm integral equations of the second kind and presented their numerical results for the stress intensity factor and crack sliding displacement to show the influences of the elliptic crack parameters, the electric field, FGPM gradation, crack length, and electromechanical coupling coefficient. Dai and Wang (2004) attempted finite integral and Laplace transforms, and their inverse transforms, and obtained the exact expression for the dynamic responses of stress, electric displacement, and electric potentials. Wang et al. (2005) developed the dynamic solution for a multilayered, spherically isotropic piezoelectric hollow sphere subjected to radial dynamic loads by dividing the problem into quasi-static and dynamic parts, and they solved the Volterra integral equation using the interpolation method. Ebrahimi et al. (2008) investigated an analytical solution for the free vibration of a moderately thick, circular functionally graded (FG) plate integrated with two thin piezoelectric layers. Based on the Mindlin plate theory, they solved the equations of motion for clamped and simply supported edge boundary conditions. Wang and Xu (2010) used the Frobenius series method to solve the second-order ordinary differential equation with variable coefficients, and they obtained the closed-form displacement solution for an exponentially graded piezoelectric spherical structure subjected to mechanical and electric loads. Dai et al. (2007) investigated the electromagnetoelastic behavior of a FGPM cylinder and sphere placed in a uniform magnetic field, which were subjected to external pressure and electric loading. They showed the sensible influence of being inhomogeneous. They also indicated a specific value, the inhomogeneity parameter or power law index, β, optimizing the electromagnetoelastic responses. Ghorbanpour Arani et al. (2008) calculated the response of magnetothermoelastic stress and perturbation of the magnetic field vector for a thick-walled, spherical FGM vessel, using Henkel and Laplace transform techniques.

Using the infinitesimal theory of piezoelasticity, Dai et al. (2010a, 2010b) presented an analytical solution for electromechanical stresses and electromagnetothermoelastic behaviors of stationary FGPM hollow cylindrical and spherical structures. The materials' properties were assumed as an identical power function in the radial direction. Li et al. (2010) treated the axisymmetric electroelastic problem of a hollow, radially polarized FGPM cylinder. They showed that β strongly affected the electric and mechanical outputs. Galic and Horgan (2003) set an analytical solution to the axisymmetric problem of an infinitely long, radially polarized, and orthotropic piezoelectric hollow cylinder rotating about its axis at a constant angular velocity. An analogy was investigated in the case of stress singularities at the origin for piezoelectric solids to those occurring in the purely mechanical problem for radially orthotropic elastic materials. Babaei and Chen (2008) generalized this problem to a functionally graded piezoelectric and studied the influence of inhomogeneity on the responses. Ghorbanpour Arani et al. (2010) considered a hollow circular cylinder made of exponentially graded piezoelectric material (EGPM), such as PZT-4 under the following conditions: loadings composed of internal and external pressures, steady-state heat conduction with convective boundary condition, rotation with constant angular velocity, and a constant electric potential difference between inner and outer surfaces. They also assumed that the material properties, except for Poisson's ratio and the thermal conduction coefficient, were exponentially distributed along radius.

In this study, the shaft is placed in a uniform axial magnetic field, and we examine the effect of the magnetic field in addition to mechanical and electric loads on the responses. All material, electrical, and

magnetic properties were assumed to follow an identical power law in the radial direction.

2. Basic formulations and governing equations

Consider an infinitely long FGPM hollow shaft that is placed in a uniform axial magnetic field, $\vec{H}(0,0,H_z)$, and subjected to pressure and electrical loading (Figure 1). The inner and outer radii of the shaft are a and b, respectively. The shaft is rotating around its axis with constant angular velocity ω. We assume that all material, magnetic permeability, and dielectric constants follow an identical power law in the radial direction. Therefore, in the cylindrical coordinate (r,θ,z) we have:

$$\begin{gathered} c_{ij}(r) = c_{ij}^0(\frac{r}{b})^\beta, \\ \mu(r) = \mu_0(\frac{r}{b})^\beta, \\ e_{ri}(r) = e_{ri}^0(\frac{r}{b})^\beta, \qquad i = r,\theta; j = r,\theta, \\ \varepsilon_{rr}(r) = \varepsilon_{rr}^0(\frac{r}{b})^\beta, \\ \rho(r) = \rho_0(\frac{r}{b})^\beta, \end{gathered} \tag{1}$$

where c_{ij} is the elastic constant, μ stands for permeability, e_{ri} is the piezoelectric constant, and ε_{rr} and ρ represent the dielectric constant and density, respectively.

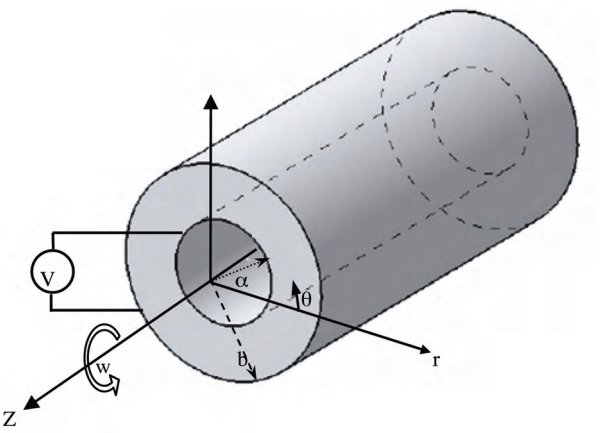

Figure 1. Configuration of a FGPM hollow shaft in axial magnetic field.

The constitutive equations for the plane strain problem of an orthotropic, radially polarized FGPM can be expressed as (Galic and Horgan, 2003):

$$\sigma_{rr} = c_{rr}\frac{\partial u}{\partial r} + c_{r\theta}\frac{u}{r} + e_{rr}\frac{\partial \psi}{\partial r}, \tag{2a}$$

$$\sigma_{\theta\theta} = c_{r\theta}\frac{\partial u}{\partial r} + c_{\theta\theta}\frac{u}{r} + e_{r\theta}\frac{\partial \psi}{\partial r}, \tag{2b}$$

$$D_{rr} = e_{rr}\frac{\partial u}{\partial r} + e_{r\theta}\frac{u}{r} - \varepsilon_{rr}\frac{\partial \psi}{\partial r}, \tag{2c}$$

where D_r is radial electric displacement and ψ represents electric potential.

The equilibrium equation and Maxwell equation in the absence of body forces and free charge density for the FGPM shaft is expressed as (Galic and Horgan, 2003; Dai and Wang, 2004):

$$\frac{\partial \sigma_r}{\partial r} + \frac{\sigma_r - \sigma_\theta}{r} + \rho\omega^2 r + f_z = 0, \tag{3}$$

$$\frac{\partial D_r}{\partial r} + \frac{D_r}{r} = 0, 0 \le r \le a, \tag{4}$$

$$h_z = -H_z\left(\frac{\partial u_r}{\partial r} + \frac{u_r}{r}\right), \tag{5}$$

where h_z is the perturbation of the magnetic field vector and f_z is defined as Lorentz's force, which may be written as:

$$f_z = \mu(r)H_z^2\frac{\partial}{\partial r}\left(\frac{\partial u}{\partial r} + \frac{u}{r}\right). \tag{6}$$

Substituting Eqs. (1), (2), and (6) into Eq. (3), the equilibrium equation will be:

$$\begin{array}{l} r^2\frac{\partial^2 u}{\partial r^2} + r\left(1 + \frac{\beta c_{rr}^0}{c_{rr}^0 + \mu_0 H_z^2}\right)\frac{\partial u}{\partial r} + \left(\frac{\beta c_{r\theta}^0 - c_{\theta\theta}^0 - \mu_0 H_z^2}{c_{rr}^0 + \mu_0 H_z^2}\right)u + r^2\left(\frac{e_{rr}^0}{c_{rr}^0 + \mu_0 H_z^2}\right)\frac{\partial^2 \psi}{\partial r^2} \\ + r\left(\frac{e_{rr}^0(\beta+1) - e_{r\theta}^0}{c_{rr}^0 + \mu_0 H_z^2}\right)\frac{\partial \psi}{\partial r} + \frac{\rho_0\omega^2 r^3}{c_{rr}^0 + \mu_0 H_z^2} = 0. \end{array} \tag{7}$$

Substituting Eqs. (1) and (2) into Eq. (4), the charge equation of electrostatics is expressed as:

$$r^2\frac{\partial^2 u}{\partial r^2} + r\left((\beta+1) + \frac{e_{r\theta}^0}{e_{rr}^0}\right)\frac{\partial u}{\partial r} + \beta\frac{e_{r\theta}^0}{e_{rr}^0}u - r^2\frac{\varepsilon_{rr}^0}{e_{rr}^0}\frac{\partial^2 \psi}{\partial r^2} - r(\beta+1)\frac{\varepsilon_{rr}^0}{e_{rr}^0}\frac{\partial \psi}{\partial r} = 0. \tag{8}$$

A new potential function is therefore defined as:

$$\Psi = \frac{e_{rr}^0}{c_{rr}^0}\psi, \tag{9}$$

For a hollow shaft with $a \le r \le b$, the dimensionless parameters are written as follows:

$$\rho = \frac{r}{a}, \tag{10}$$

$$\eta = \frac{b}{a}, \tag{11}$$

Therefore, $1 \le \rho \le \eta$, and with regard to Eqs. (9), (10), and (11) and using the chain rule for derivatives, we can rewrite Eqs. (7) and (8) in the following forms:

$$\rho^2\frac{\partial^2 u}{\partial \rho^2} + (1 + \beta\xi)\rho\frac{\partial u}{\partial \rho} + \Gamma u + \xi\rho^2\frac{\partial^2 \Psi}{\partial \rho^2} + (\beta + 1 - \alpha)\xi\rho\frac{\partial \Psi}{\partial \rho} = -\Omega a\rho^3, \tag{12}$$

$$\rho^2\frac{\partial^2 u}{\partial \rho^2} + (\beta + 1 + \alpha)\rho\frac{\partial u}{\partial \rho} + \beta\alpha u - \gamma\rho^2\frac{\partial^2 \Psi}{\partial \rho^2} - \gamma(\beta+1)\rho\frac{\partial \Psi}{\partial \rho} = 0, \tag{13}$$

$$\xi = \frac{c_{rr}^0}{c_{rr}^0 + \mu_0 H_z^2}, \tag{14a}$$

$$\Gamma = \frac{\beta c_{r\theta}^0 - c_{\theta\theta}^0 - \mu_0 H_z^2}{c_{rr}^0 + \mu_0 H_z^2}, \tag{14b}$$

$$\alpha = \frac{e_{r\theta}^0}{e_{rr}^0}, \tag{14c}$$

$$\Omega = \frac{\rho_0 \omega^2 a^2}{c_{rr}^0 + \mu_0 H_z^2}, \tag{14d}$$

$$\gamma = \frac{\varepsilon_{rr}^0 c_{rr}^0}{e_{rr}^{0\ 2}}. \tag{14e}$$

Assuming $\rho = e^t$, the solutions for Eqs. (12) and (13) are obtained as:

$$u'' + \beta\xi u' + \Gamma u + \xi\Psi'' + \xi(\beta - \alpha)\Psi' = -\Omega a e^{3t}, \tag{15}$$

$$u'' + (\beta + \alpha)u' + \beta\alpha u - \gamma\Psi'' - \gamma\beta\Psi' = 0, \tag{16}$$

where u' and ψ' correspond to the differentiation of displacement and electric potential with respect to t. We can decouple this system by eliminating ψ'' between Eqs. (15) and (16) and determine the value of ψ' . We therefore have:

$$\Psi' = A_2 u'' + A_1 u' + A_0 u + d, \tag{17}$$

$$A_2 = \frac{\gamma + \xi}{\gamma\xi\alpha}, \tag{18}$$

$$A_1 = \frac{\beta(\gamma + 1) + \alpha}{\gamma\alpha}, \tag{19}$$

$$A_0 = \frac{\gamma\Gamma + \xi\beta\alpha}{\gamma\xi\alpha}, \tag{20}$$

$$d = \frac{\Omega a e^{3t}}{\xi\alpha}. \tag{21}$$

By substituting Eq. (17) and its derivative into Eq. (15), we have:

$$B_4 u''' + B_3 u'' + B_2 u' + B_1 u + B_0 e^{3t} = 0, \tag{22}$$

where:

$$B_4 = \frac{\gamma + \xi}{\gamma\alpha}, \tag{23a}$$

$$B_3 = \frac{\beta(\gamma(1 + \xi) + 2\xi)}{\gamma\alpha}, \tag{23b}$$

$$B_2 = \frac{\Gamma}{\alpha} + \frac{\xi(\beta\alpha + \beta^2(\gamma + 1) - \alpha^2)}{\gamma\alpha}, \tag{23c}$$

$$B_1 = \frac{\beta\Gamma}{\alpha} + \frac{\beta\xi(\beta-\alpha)}{\gamma}, \tag{23d}$$

$$B_0 = \frac{(3+\beta)\Omega a}{\alpha}. \tag{23e}$$

To determine the solution for Eq. (22), we must first obtain the homogeneous term of the solution. We can express this term as:

$$u_g = Ae^{m_1 t} + Be^{m_2 t} + Ce^{m_3 t}, \tag{24}$$

where m_1, m_2, and m_3 are the roots of the characteristic equation of Eq. (22) and A, B, and C are obtained by satisfying the boundary conditions. Assuming $u_p = Ke^{3t}$ for a particular term of the solution and by substituting it into Eq. (22), K can be determined as follows:

$$K = \frac{-B_0}{27B_4 + 9B_3 + 3B_2 + B_1}. \tag{25}$$

Therefore, the solution of Eq. (22) can be defined as:

$$u = u_g + u_p \Rightarrow u = A\rho^{m_1} + B\rho^{m_2} + C\rho^{m_3} + K\rho^3. \tag{26}$$

We can also obtain ψ by using Eq. (17).

$$\Psi = H_1 A\rho^{m_1} + H_2 B\rho^{m_2} + H_3 C\rho^{m_3} + H_4\rho^3 + D, \tag{27}$$

where:

$$H_i = A_2 m_i + A_1 + \frac{A_0}{m_i}, \qquad i = 1, 2, 3, \tag{28a}$$

$$H_4 = K(3A_2 + A_1 + \frac{A_0}{3}) + \frac{\Omega a}{3\xi\alpha}. \tag{28b}$$

The nondimensionalized form of stresses is hence obtained from Eqs. (2a) and (2b), which is written as:

$$\frac{\sigma_{rr}}{c^{\circ}_{rr}} = \frac{1}{a}[\frac{c_{rr}}{c^{\circ}_{rr}}\frac{du}{d\rho} + \frac{c_{r\theta}}{c^{\circ}_{rr}}\frac{u}{\rho} + \frac{e_{rr}}{c^{\circ}_{rr}}\frac{d\psi}{d\rho}], \tag{29}$$

$$\frac{\sigma_{\theta\theta}}{c^{\circ}_{rr}} = \frac{1}{a}[\frac{c_{r\theta}}{c^{\circ}_{rr}}\frac{du}{d\rho} + \frac{c_{\theta\theta}}{c^{\circ}_{rr}}\frac{u}{\rho} + \frac{e_{r\theta}}{c^{\circ}_{rr}}\frac{d\psi}{d\rho}]. \tag{30}$$

Substituting Eqs. (26) and (27) into Eqs. (29) and (30) yields the dimensionless stresses and the potential Ψ_1, as follows:

$$\begin{aligned}\frac{\sigma_{rr}}{c^{\circ}_{rr}} &= \tfrac{1}{a}\eta^{-\beta}\rho^{\beta}[A\rho^{m_1-1}(m_1(1+H_1)+\delta) + B\rho^{m_2-1}(m_2(1+H_2)+\delta) + C\rho^{m_3-1}(m_3(1+H_3)+\delta) \\ &\quad +\rho^2(K(3+\delta)+3H_4)],\end{aligned} \tag{31}$$

$$\begin{aligned}\frac{\sigma_{\theta\theta}}{c^{\circ}_{rr}} &= \tfrac{1}{a}\eta^{-\beta}\rho^{\beta}[A\rho^{m_1-1}(m_1(\delta+\alpha H_1)+\upsilon) + B\rho^{m_2-1}(m_2(\delta+\alpha H_2)+\upsilon) + C\rho^{m_3-1}(m_3(\delta+\alpha H_3)+\upsilon) \\ &\quad +\rho^2(K(3\delta+\upsilon)+3H_4\alpha)],\end{aligned} \tag{32}$$

$$\delta = \frac{c^0_{r\theta}}{c^0_{rr}}, \tag{33}$$

$$\nu = \frac{c^0_{\theta\theta}}{c^0_{rr}}. \tag{34}$$

As for the dimensionless potential Ψ_1, we have:

$$\Psi_1 = \frac{\Psi}{a}, \tag{35}$$

$$\Psi_1 = \frac{1}{a}(H_1 A\rho^{m_1} + H_2 B\rho^{m_2} + H_3 C\rho^{m_3} + H_4\rho^3 + D), \tag{36}$$

Now the boundary conditions are applied to determine the integral constants A, B, C, and D in Eqs. (27), (31), and (32). We can write the result of each case in matrix form, such as $MX = Y$ where M is a 4×4 matrix, X is [A, B, C, D], and Y is a 4×1 matrix.

3. Numerical results

In the previous section, we obtained the analytical solutions for a rotating FGPM shaft in a magnetic field. In this section, we study the numerical results for a typical FGPM shaft. We assume that the exterior surface is made of piezoelectric PZT-4. The properties of this important piezoelectric material are listed in the Table.

Table. Material constants of PZT-4 (Galic and Horgan, 2003).

PZT-4	
$c^0_{rr} = 115 \times 10^9 Pa$	$c^0_{r\theta} = 74.3 \times 10^9 Pa$
$c^0_{\theta\theta} = 139 \times 10^9 Pa$	$e^0_{rr} = 15.1 c/m^2$
$e^0_{r\theta} = -5.2 c/m^2$	$\varepsilon^0_{rr} = 5.62 \times 10^{-9} c^2/Nm^2$
$\rho_0 = 7.5 \times 10^3 kg/m^3$	$\mu_0 = 4\pi \times 10^{-7} H/m$

Example 1. Suppose a rotating FGPM shaft is subjected only to internal pressure with neither electric potential nor magnetic fields. Thus, in the $r = a$ $(\rho = 1)$ and $r = b$ $(\rho = \beta)$, we have:

$$\frac{\sigma_{rr}}{c^\circ_{rr}}(1) = -1, \frac{\sigma_{rr}}{c^\circ_{rr}}(\eta) = 0, \Psi_1(1) = 0, \Psi_1(\eta) = 0, H_z = 0. \tag{37}$$

To demonstrate the effect of β, the internal pressure is normalized to unity. Radial and circumferential stresses as well as electric potential distributions are shown in Figure 2. The diagram of radial stress satisfies the boundary conditions. According to the circumferential stress diagram, in $\rho \approx 2.85$, for all values of β, the stress is the same. Furthermore, as β is increased, the dimensionless radial stress is reduced. As for the electric potential, as β is increased, Ψ_1 shifts from negative to positive values. Moreover, it can be concluded from Figure 2 that the β exponent significantly affects the induced electric potential.

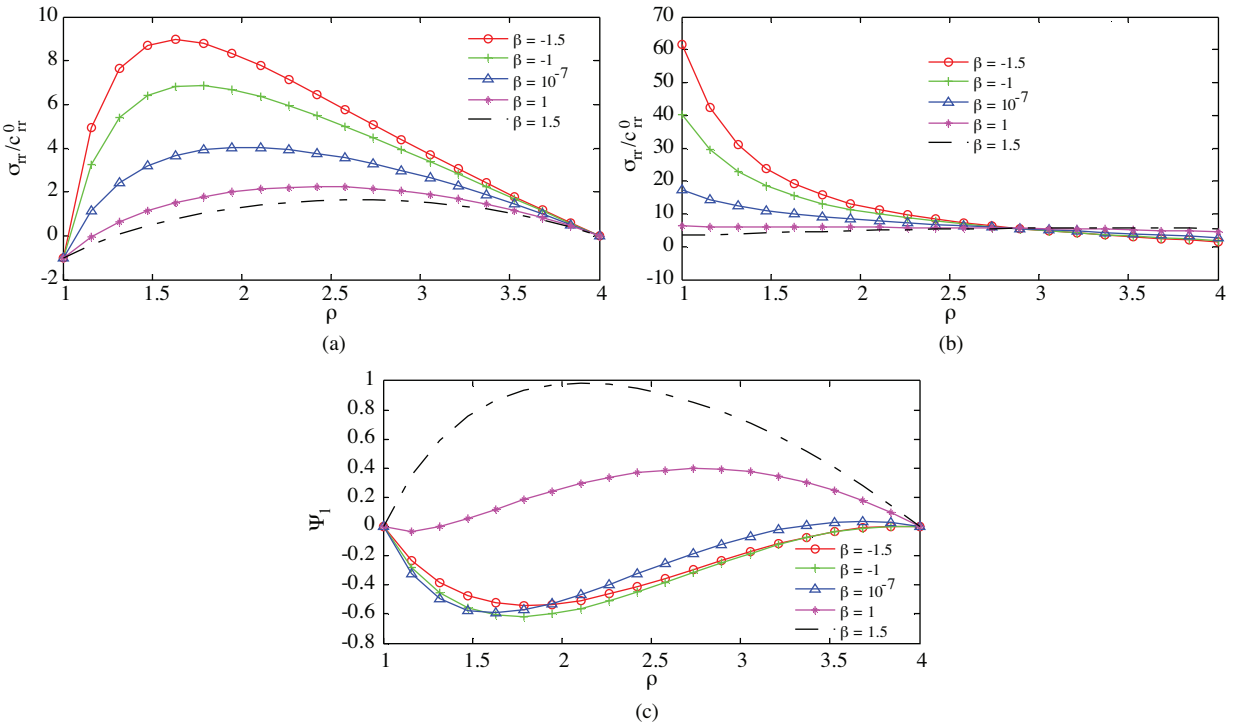

Figure 2. a) Radial stress, b) circumferential stress, and c) electric potential distributions versus the dimensionless parameter ρ for example 1: $\mathrm{H}_z = 0$, $\Omega = 1$.

Example 2. Consider a rotating FGPM shaft that is subjected only to an electric potential without any mechanical load or magnetic field. We thus have:

$$\frac{\sigma_{rr}}{c^{\circ}_{rr}}(1) = 0, \frac{\sigma_{rr}}{c^{\circ}_{rr}}(\eta) = 0, \Psi_1(1) = 1, \Psi_1(\eta) = 0, H_z = 0. \tag{38}$$

Figure 3 also shows radial and circumferential stresses as well as the electric potential for this case. The diagram of electric potential satisfies the boundary conditions. As in example 1, for $\rho \approx 3.15$, for all values of β, the stress is the same and the dimensionless radial stress is reduced as β increases. As far as the electric potential is concerned, β increasing shifts Ψ_1 from negative to positive values, but compared to the previous example, the maximum is considerably higher.

Example 3. Here, a rotating FGPM shaft is considered that is subjected to internal pressure and electric potential, but no magnetic field. Again we have:

$$\frac{\sigma_{rr}}{c^{\circ}_{rr}}(1) = -1, \frac{\sigma_{rr}}{c^{\circ}_{rr}}(\eta) = 0, \Psi_1(1) = 1, \Psi_1(\eta) = 0, H_z = 0. \tag{39}$$

Figure 4 shows the results for example 3. Radial stress and electric potential diagrams satisfy the imposed boundary conditions. These results coincide with those obtained by Galic and Horgan (2003) ($\beta = 10^{-7} \approx 0$) and Babaei and Chen (2008), and this validates the responses obtained in this study.

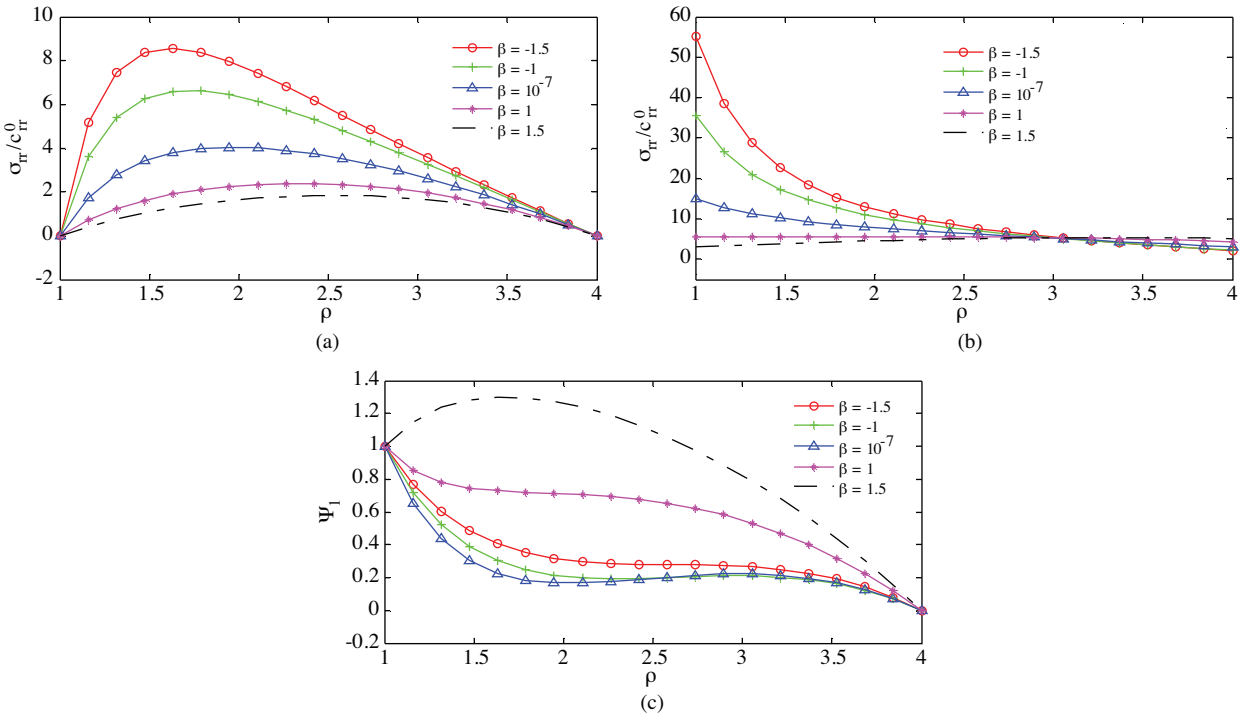

Figure 3. a) Radial stress, b) circumferential stress, and c) electric potential distributions versus the dimensionless parameter ρ for example 2: $H_z = 0$, $\Omega = 1$.

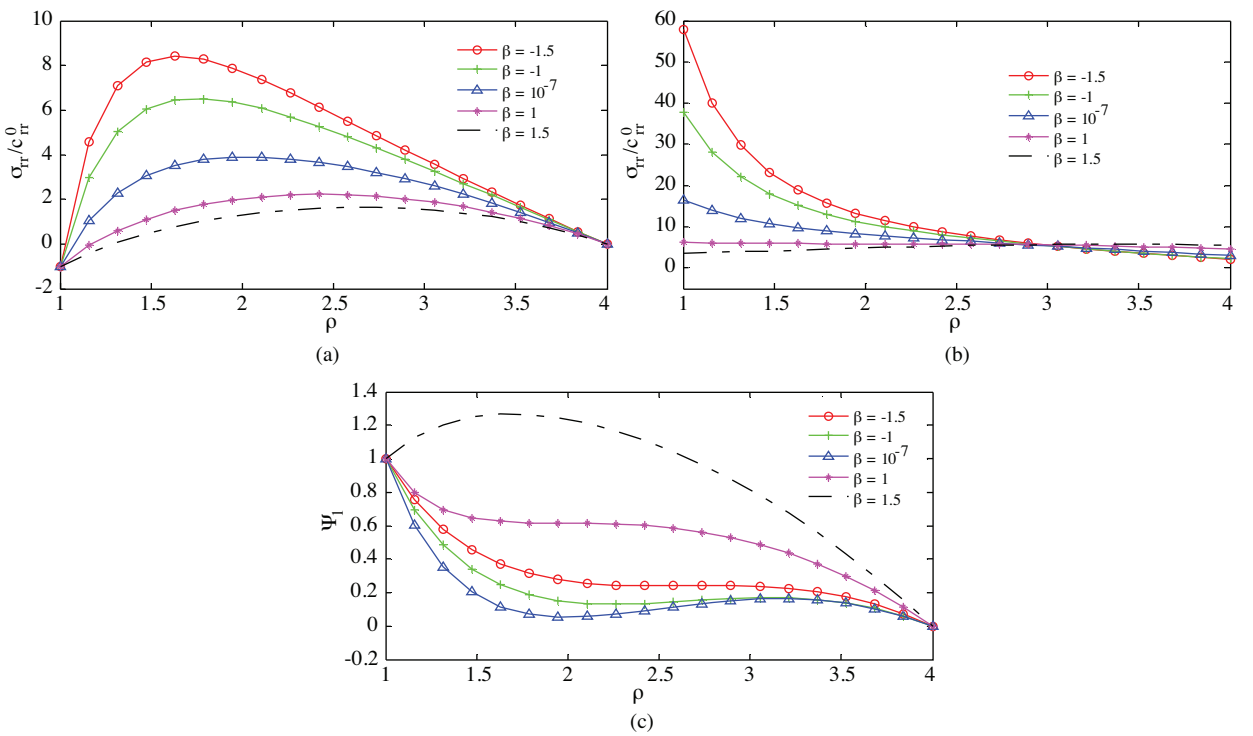

Figure 4. a) Radial stress, b) circumferential stress, and c) electric potential distributions versus the dimensionless parameter ρ for example 3: $H_z = 0$, $\Omega = 1$.

Example 4. This case is the superposition of examples 1, 2, and 3. A rotating FGPM shaft is subjected to internal pressure and electric potential and is placed in a uniform axial magnetic field. The corresponding boundary conditions could be expressed as:

$$\frac{\sigma_{rr}}{c^{\circ}_{rr}}(1) = -1, \frac{\sigma_{rr}}{c^{\circ}_{rr}}(\eta) = 0, \Psi_1(1) = 1, \Psi_1(\eta) = 0, H_z = 1.796 \times 10^9 A/m. \tag{40}$$

Comparing Figure 5 with Figure 4 indicates that the effects of the magnetic field on dimensionless radial and circumferential stresses are almost double in Figure 5.

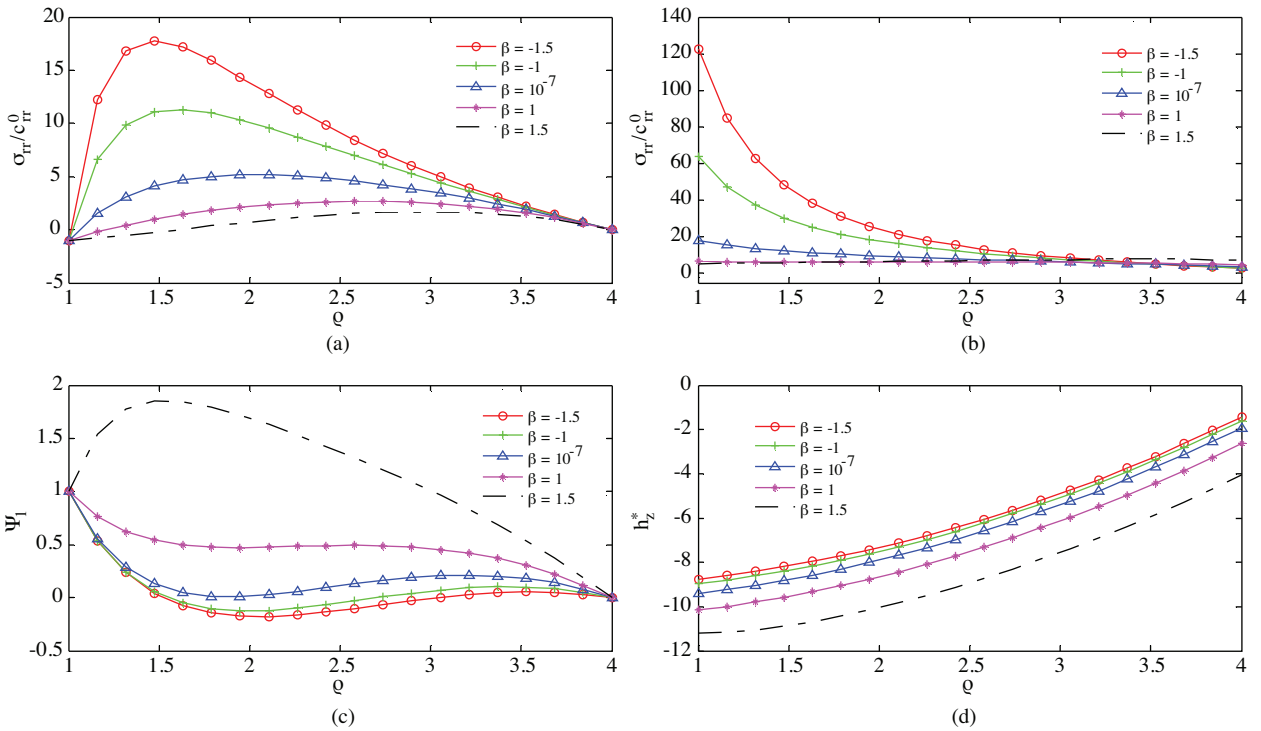

Figure 5. a) Radial stress, b) circumferential stress, c) electric potential, and d) the perturbation of magnetic field vector distributions versus the dimensionless parameter $\rho$for example 4: $H_z = 1.796 \times 10^9$ A/m, $\Omega = 1$.

4. Conclusions

In this paper, the electromagnetomechanical responses of a radially polarized rotating shaft made of FGPM and subjected to a uniform magnetic field with mechanical and electric potentials were studied. All material, electrical, and magnetic properties were assumed to follow an identical power law in the radial direction. Using the infinitesimal theory of electromagnetoelasticity, exact solutions for electric displacement, stresses, electric potentials, and perturbation of the magnetic field vector were obtained. Dimensionless circumferential stress for different values of β seemed to be almost constant as ρ increased. However, the dimensionless radial stress was reduced by increasing β. These results conform to those presented by Galic and Horgan (2003) ($\beta = 10^{-7} \approx 0$) and Babaei and Chen (2008), indicating the validation of the responses obtained here. Moreover, in the presence of the magnetic field, dimensionless radial and circumferential stresses increased almost 2-fold. Results further indicated that the β exponent significantly affected the radial and circumferential stress distributions and the

electric potential and magnetic field. This implies that the electromagnetomechanical fields in the rotating shaft should be optimized for any specific application by selecting the appropriate β exponent.

Nomenclature

ω	angular velocity	D_r	radial electric displacement
r	radial variable	Ψ	electric potential
θ	circumferential variable	h_z	perturbation of magnetic field vector
β	inhomogeneity parameter or power law index	f_z	Lorentz's force
c_{ij}	elastic constant	ρ	mass density
μ	magnetic permeability	σ_{rr}, $\sigma_{\theta\theta}$	components of stresses
e_{ri}	piezoelectric constant	a, b	inner and outer radii
ε_{rr}	dielectric constant		

References

Adelman, N.T., Stavsky, Y. and Segal, E., "Axisymmetric Vibrations of Radially Polarized Piezoelectric Ceramic Cylinders", J. Sound and Vibration, 38, 245-254, 1975.

Babaei, M.H. and Chen, Z.T., "Analytical Solution for the Electromechanical Behavior of a Rotating Functionally Graded Piezoelectric Hollow Shaft", Archive of Applied Mechanics, 78, 489-500, 2008.

Chen, W.Q., "Problems of Radially Polarized Piezoelastic Bodies", Int. J. Solids & Structures, 36, 4317-4332, 1999.

Dai, H.L., Fu, Y.M. and Yang, J. H., "Electromagnetoelastic Behaviors of Functionally Graded Piezoelectric Solid Cylinder and Sphere", Acta Mechanica Sinica, 23, 55-63, 2007.

Dai, H.L., Hong, L., Fu, Y.M. and Xiao, X., "Analytical Solution for Electromagnetothermoelastic Behaviors of a Functionally Graded Piezoelectric Hollow Cylinder", Applied Mathematical Modelling, 34, 343-357, 2010a.

Dai, H.L. and Wang, X., "Dynamic Responses of Piezoelectric Hollow Cylinder in an Axial Magnetic Field", Int. J. Solids and Structures, 41, 5231-5246, 2004.

Dai, H.L., Xiao, X. and Fu, Y.M., "Analytical Solutions of Stresses in Functionally Graded Piezoelectric Hollow Structures", J. Solid State Communications, 150, 763-767, 2010b.

Ebrahimi, F., Rastgoo, A. and Kargarnovin, M.H., "Analytical Investigation on Axisymmetric Free Vibrations Of Moderately Thick Circular Functionally Graded Plate Integrated with Piezoelectric Layers", J. Mechanical Science and Technology, 22, 1058-1072, 2008.

Galic, D. and Horgan, C.O., "The Stress Response of Radially Polarized Rotating Piezoelectric Cylinders", J. Applied Mechanics, 70, 426-435, 2003.

Ghorbanpour Arani, A., Loghman, A., Abdollahitaheri, A. and Atabakhshian, V., "Electro-Thermo-Mechanical Behaviors of a Radially Polarized Rotating Functionally Graded Piezoelectric Cylinder", Journal of Mechanics of Materials and Structures, 2010, in press.

Ghorbanpour Arani, A., Salari, M., Khademizadeh, H. and Arefmanesh, A., "Magnetothermoelastic Transient Response of a Functionally Graded Thick Hollow Sphere Subjected to Magnetic and Thermoelastic Fields", Archive of Applied Mechanics, 79, 481-497, 2008.

Jabbari, M., Sohrabpour, S. and Eslami, M.R., "Mechanical and Thermal Stresses in a Functionally Graded Hollow Cylinder Due to Radially Symmetric Loads", Int. J. Pressure Vessels and Piping, 79, 493-497, 2002.

Kwon, S.M. and Lee, K.Y., "Dynamic Response of an Anti-Plane Shear Crack in a Functionally Graded Piezoelectric Strip", Journal of Mechanical Science & Technology, 18, 419-431, 2004.

Li, X.F., Peng, X.L. and Lee, K.Y., "Radially Polarized Functionally Graded Piezoelectric Hollow Cylinders as Sensors and Actuators", European Journal of Mechanics A/Solids, 29, 704-713, 2010.

Wang, H.M., Ding, H.J. and Chen, Y.M., "Transient Responses of a Multilayered Spherically Isotropic Piezoelectric Hollow Sphere", Archive of Applied Mechanics, 74, 581-599, 2005.

Wang, H.M. and Xu, Z.X., "Effect of Material Inhomogeneity on Electromechanical Behaviors of Functionally Graded Piezoelectric Spherical Structures", Computational Materials Science, 48, 440-445, 2010.

Wu, X.H., Chen, C., Shen, Y.P. and Tian, X.G., "A High Order Theory for Functionally Graded Piezoelectric Shells", Int. J. Solids and Structures, 39, 5325-5344, 2002.